MODELING AND SIMULATION OF THE SUPERREGENERATIVE RECEIVER

Rodolfo Feick and Osvaldo Rojas
Departamento de Electrónica, Universidad Técnica Federico Santa María
P.O. Box 110-V, Valparaíso, Chile
e-mail: rfl@elo.utfsm.cl

Alejandro Mackay, Departemento de Ingeniería Eléctrica, Pontificia Universidad Católica de Chile

Abstract

This paper presents a model for the super-regenerative receiver, a device widely used in short distance telemetry and remote control applications. The difficulty in modeling this nonlinear and time varying device by traditional analytic tools has meant that to this date, results based on a much simplified description of the circuit have been used as the basis for design. In this paper we show how with the aid of modern computer based analysis and simulation tools, a much more general characterization of the behavior of the receiver is possible.

1. INTRODUCTION

The superregenerative receiver [1], [2], [3], [4], [5] has been used for many decades and is still manufactured in large quantities for short range data link applications such as auto alarm systems, garage door openers etc. While the basic design has not been modified since its inception, advances in electronic devices have resulted in some changes in the implementation of the circuit.

Among the reasons for the superregenerative receiver's popularity are high gain with very few active components, simplicity, low cost and low power consumption. Another quite interesting aspect is the property of a constant demodulated output over a very wide range of input signal levels.

The superregenerative receiver has some well known shortcomings that basically relate to its inherent frequency instability. A fairly recent work [6] reports on a design that uses a narrowband SAW device to stabilize the receiver.

While the receiver has continued to be extensively used, it's analytical treatment was virtually abandoned after the pioneering works of Armstrong and Frink [1], [2]. Although the receiver is extremely simple in its basic design, a thorough analysis is quite complex due to the time varying and nonlinear characteristics of the circuit. The results obtained from the simplified model that has served as the basis for the analysis, are still quoted in the literature for the prediction of the behavior of more complex circuits [6], [7], and "cut and try" based design is extensively used [8].

The availability of modern computer based analytical tools and simulators allows a much more precise characterization of the basic receiver and of its variants.

In this paper we present a treatment of the super-regenerative receiver that extends some of the basic and well known relations describing its behavior, to more complex and realistic configurations than those discussed in the classical literature. The treatment is based on a theoretical analysis, complemented by the use of computer based tools. Situations that do not lend themselves to an analytical treatment are discussed with the aid of simulation results. It is shown that several relations obtained from the analysis of the basic circuit, can be extended to the more complex configurations that describe a real implementation. The general approach is based on a block diagram model of the receiver. The design parameters considered are not component values as in the classical circuit based analysis [2], [5] but block parameters such as filter bandwidth and amplifier gain. While any practical implementation will in general only approximately match a block diagram, the results obtained provide a systematic guide that defines the complex interrelation between the various parameters.

As a result of this work, criteria that take some of the guesswork out of the design of a superregenerative receiver have been obtained.

2. ANALYSIS OF THE BASIC SUPERREGENERATIVE RECEIVER

The configuration of a typical superregenerative receiver at the block diagram level is shown in Fig. 1.

Contributed Paper

Manuscript received January 31, 1997

0098 3063/97 $10.00

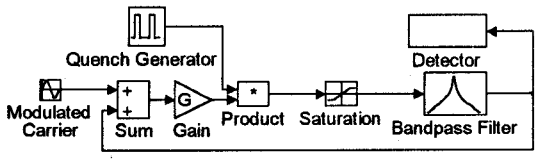

Figure 1: Block diagram of receiver

The operation principle of the receiver is well known: The quench oscillator generates a sequence of intervals during which the closed loop alternates between periods of oscillation and periods of oscillation quenching. The amplitude of the input carrier modulates the width of the oscillation pulses, the amplitude of which is determined by the saturation of the active device. The detector responds to the average pulse duration. The condition resulting in saturation of the oscillation pulses, known as the "logarithmic mode" is the normal operating mode for this type of receiver, and is the only one that will be discussed here. As is obvious, the quench frequency must be much larger than the highest frequency of the carrier modulation, in order to be able to eliminate it by low pass filtering. We will only consider the case where the quench frequency is fixed, independent of the carrier level, the "externally quenched" receiver.

The relation between the output voltage variation of a superregenerative receiver operating in the logarithmic mode, and the corresponding input signal modulation, has been discussed in the literature assuming a simple RLC series loop [2], [5]. The well known results are repeated here only for reference purposes.

We assume that the oscillations of the loop are switched on and off at a fixed rate f_q, the quench frequency. We further assume that the envelope of the oscillations grows exponentially, with a time constant τ, reaching a saturation level E_{max} at the filter output. If the input signal voltage varies between V_1 and V_2, then it has been shown [5], that for the RLC type loop, the demodulated output voltage varies in a range V given by:

$$V = f_q E_{max} \tau \ln\left(\frac{V_2}{V_1}\right) \qquad (1)$$

For an input signal that varies in a range $V_a - \Delta V$ to $V_a + \Delta V$ we can define a modulation index $m = \Delta V / V_a$ and rewrite (1) as:

$$V = f_q E_{max} \tau \ln\left(\frac{1+m}{1-m}\right) \qquad (2)$$

As can be seen from (2), a very attractive feature of the superregenerative receiver is the fact that it's demodulated output does not depend on the average received signal power, a behavior equivalent to an extremely efficient automatic gain control. This behavior has been justified on the basis of the analysis of the exponential growth of the oscillation pulses for the simple series RLC loop. We will here examine this aspect in a more general form.

The demodulated signal output varies in proportion to the area under the oscillation pulses. Since the decay of the pulses from the saturation level does not depend on the input signal, the variation in area is only dependent on the behavior during the growth phase. For this discussion we will assume that the quench waveshape is rectangular, and thus, that the amplifier is periodically switched on and off. The growth of the oscillation pulses, before saturation effects become significant, then corresponds to the behavior of a linear time invariant system, with an initial condition determined by the input signal level at the time the oscillation starts. For a circuit that generates exponentially growing pulses, variations in the initial condition only produce a time shift in the pulse buildup phase, without altering its shape [5]. This time shift t_a, the "time of advance", is responsible for the increase in pulse width and thus the increase in the demodulated output. We will show that the exponential growth of the oscillation pulses to saturation is not only a sufficient but also a necessary condition for the constant demodulated output.

Let V_1 and $V_2 > V_1$ be two initial conditions and let t_a be the time of advance produced by the increase from V_1 to V_2. If the demodulated signal is to be only a function of the amplitude modulation index, the time of advance must only depend on the ratio of the initial conditions and not on the absolute signal level. Let p(t) describe the envelope of a pulse resulting from an initial condition V_{in}, at time t=0. Then for the time interval previous to the onset of saturation we can write:

$$p(t) = V_{in} f(t) \qquad (3)$$

Our requirement for a time of advance t_a that only depends on the ratio of initial conditions then becomes:

$$V_1 f(t) = V_2 f(t + t_a)$$

$$\text{with } t_a \text{ a function of } \frac{V_1}{V_2} \qquad (4)$$

(4) can be rewritten as:

$$f(t + t_a) = K(t_a)f(t) \quad \text{for all t before saturation of amplifier} \tag{5}$$

and we can thus write:

$$f(t + \Delta t) = K(\Delta t)f(t) \tag{6}$$

in any practical situation f(t) will be continuos and differentiable, and thus:

$\lim_{\Delta t \to 0} K(\Delta t) = 1$, that is K(0) = 1

and

$$f'(t) = \lim_{\Delta t \to o} \frac{f(t + \Delta t) - f(t)}{\Delta t} \tag{7}$$

Combining (6) and (7) we have:

$$f'(t) = \lim_{\Delta t \to 0} \frac{K(\Delta t) - K(0)}{\Delta t} f(t) \tag{8}$$

which can be rewritten as:

$$\frac{d}{dt} \ln\{f(t)\} = \frac{d}{dt} K(t)\Big|_{t=0} \tag{9}$$

(9) implies that $\frac{d}{dt} \ln\{f(t)\}$ is independent of t integrating and using the initial condition, we obtain a general expression for the pulse envelope p(t):

$$p(t) = V_{in} e^{\alpha t} \tag{10}$$

We have thus shown that when the system starts its oscillation in the linear range, a necessary and sufficient condition for the time of advance to depend only on the ratio of initial conditions, is the exponential growth of the oscillation pulses. Obviously this will not hold close to saturation. However as the system is still time invariant during the saturation phase, the same time shift in the growth curve will persist once the curve departs from the form defined by (10).

For the circuit configuration in figure 1, the initial condition for the oscillation is the signal voltage applied to the filter when the gain of the oscillator is switched on by the quench generator.

If the oscillation grows exponentially until saturation sets in, then the condition of constant demodulated voltage will be met.

Practical implementations of the superregenerative receiver will in general depart from the simple model treated in the literature. However in many cases the growth of the oscillations will still have an exponential envelope of the form defined by (10). To see this we consider the closed loop poles of a configuration as shown in figure 1. The oscillation condition for the loop implies that at least one pair of (complex conjugate) poles must lie to the right of the imaginary axis. We thus consider two cases:

i) Only one pair of poles in the right half plane. In this case the oscillation will grow exponentially and will contain other terms that decay exponentially and thus do not contribute to the area under the pulses in a significant way.
ii) More than one pair of unstable poles. Assume there are N such pairs of poles. The significant terms of the impulse response during the linear phase, can then be written as follows:

$$h(t) = \sum_{i=1}^{N} a_i e^{\alpha_i t} \cos(\omega_i t + \varphi_i) \tag{11}$$

The values of a_i, α_i and ω_i will depend on the position of the poles of the transfer function. In many cases the response of the loop can still be approximated by an exponentially growing envelope as in (10). In fact, if one of the coefficients α_i is significantly larger than the rest, the corresponding term will dominate the response characteristic. Even when this is not the case, the sinusoidal input signal may only excite one mode. Thus a multimode response that differs significantly from (10) is only possible if two pairs of poles are close to each other. The root locus of the closed loop system thus determines whether or not the receiver will posses the constant demodulated output voltage property. It is obviously true in general, that a loop with a high order filter is prone to generate a multimode response. A typical situation is illustrated in the following two examples that show the root locus as a function of gain, for a fourth order Butterworth filter and for an eighth order Butterworth filter. In both cases a center frequency of 100[MHz] and a bandwidth of 5[MHz] was assumed. For ease of interpretation, only the real part of the complex conjugate roots was plotted, for a relevant range of loop gain values.

As can be seen, for the fourth order filter only one pair of unstable poles exists. For the eighth order filter, there are three unstable pairs of poles as G grows. Two of them have very similar real parts, in fact they are indistinguishable in figure 3. The third pair has a real part that is considerably larger and it will thus dominate the response characteristic. As a consequence, the receiver is expected to have the constant demodulated output property.

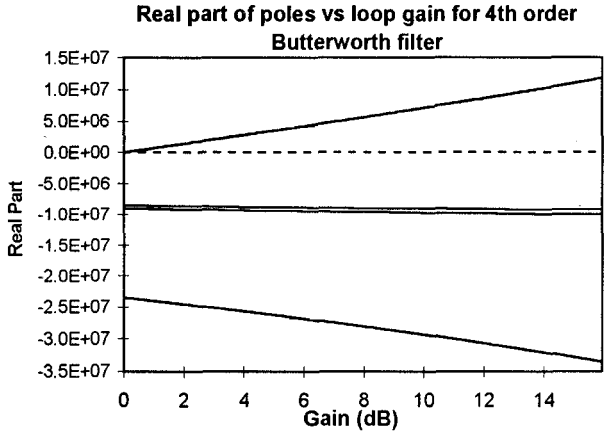

Figure 2: Real part of poles for loop with fourth order Butterworth filter

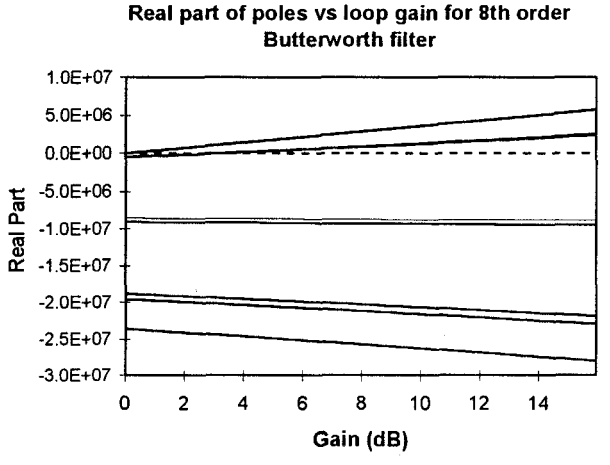

Figure 3: Real part of poles for loop with eighth order Butterworth filter

3. INFLUENCE OF QUENCH FREQUENCY

The choice of the proper quench frequency plays a crucial role in the receiver design. Too low a value implies a low gain, whereas too high a value does not assure proper quenching or saturation. The quench period only has the purpose of resetting the circuit for the next oscillation pulse, without affecting demodulated output. It should thus be made as short as feasible to be able to increase the quench frequency. The duration of the oscillation period must be such as to assure saturation, and it thus depends on the time constant τ. We will determine a bound for the quench frequency and the demodulated output, as a function of the desired dynamic range of the receiver. Let E_{sat} be the saturation voltage of the amplifier, and let E_{min} be the smallest initial condition at the filter input, i.e. at the amplifier output. Referring to the configuration of figure 1, E_{min} will be the minimum detectable signal (which will usually be determined by noise and interference), multiplied by the amplifier gain. The requirement is that starting from E_{min} an oscillation pulse will reach saturation. Let T be the required time interval. For an exponentially growing pulse, with time constant τ, the condition is:

$$T > \tau \ln\left(\frac{E_{sat}}{E_{min}}\right) \tag{12}$$

Thus for a rectangular quench waveform, the quench frequency is bounded by:

$$f_q < \frac{2}{\tau \ln\left(\frac{E_{sat}}{E_{min}}\right)} \tag{13}$$

The above condition is necessary but not sufficient, as additionally it must be ascertained that during the quench period the oscillations decay to levels that are less than the value of E_{min}. This condition will depend on the nature of the quench procedure and due to it's dependency on the circuit configuration will no be dealt with here.

Having obtained a bound on the quench frequency, it is interesting to determine how this bound limits the demodulated output.

If the saturation of the oscillation pulses reaches levels such that the output of the amplifier is essentially a square wave, then the output of the filter will be the first harmonic of this square wave and we can write:

$$E_{max} = \frac{4}{\pi} E_{sat} \tag{14}$$

It then follows from (2) (13) and (14) that the demodulated voltage V is bounded by:

$$V < \frac{2}{\ln\left(\frac{\frac{\pi}{4}E_{max}}{E_{min}}\right)} E_{max} \ln\left(\frac{1+m}{1-m}\right) \tag{15}$$

As can be seen from the above, while the maximum quench frequency is dependent on the time constant

of the closed loop response, the maximum demodulated output is not. It also follows from (12), (13) and (14) that while an increase in E_{max} forces a reduction of the quench frequency, the net result is an increase in the bound on the demodulated output.

4. INFLUENCE OF FILTER PARAMETERS

As has been discussed above, the order of the loop filter has virtually no effect on the qualitative behavior of the receiver, regarding its constant demodulated output property. However as will be seen, it has a very significant effect on the growth rate of the oscillation pulses and consequently on the admissible range of quench frequencies.

In order to observe the effect of the filter on the demodulated output, it is necessary to determine the behavior of the dominant time constant of the oscillation pulses, as a function of the filter specifications. Due to the ample range of design possibilities, it is only possible to resolve this problem on a case by case situation. The following results are based on the analysis of a loop that includes a Butterworth filter centered at 100[MHz], the order and bandwidth of which was varied. The value of the dominant time constant (if more than one pair of unstable poles exists) was determined using MATLAB. In addition an analytic expression for the impulse response was obtained using MAPLE. The same tool was used to verify that in fact the response to the carrier input is dominated by the behavior of one pair of poles.

Figure 4 shows the influence of the order of the filter N, on the dominant time constant for various values of loop gain G, maintaining the filter's bandwidth at 5[MHz]. As can be seen, an increase in the order of the filter results in an increase in the value of the time constant, the relation being quite linear.

Figure 5 illustrates the effect of reducing the bandwidth for filters of various orders. In this case it can be seen that the time constant shows an almost linear dependence on the reciprocal of the filter bandwidth.

Figure 6 illustrates the variation of the dominant time constant with loop gain for filters of various orders and bandwidths. It was found that while the curves obviously differ by a scale factor, their shape is quite similar. This indicates that the behavior of the receiver, as gain is varied, will be very similar, regardless of the order and bandwidth of the filter.

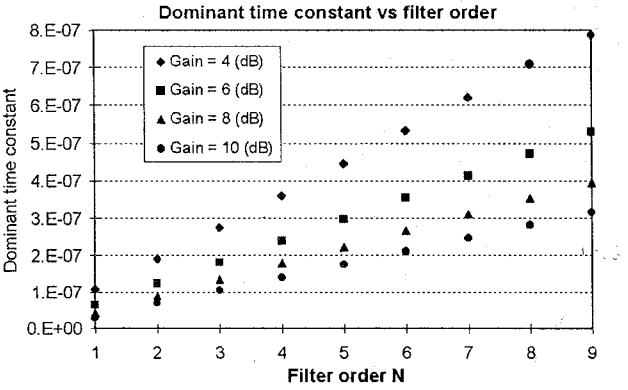

Figure 4: Dominant time constant vs. order of filter

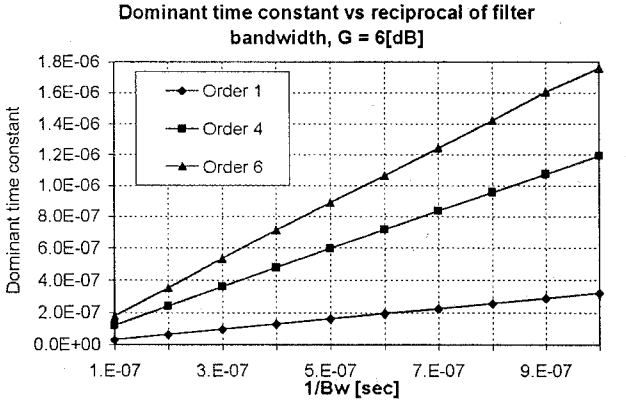

Figure 5: Dominant time constant vs. reciprocal of filter bandwidth, for a loop gain of 6 [dB]

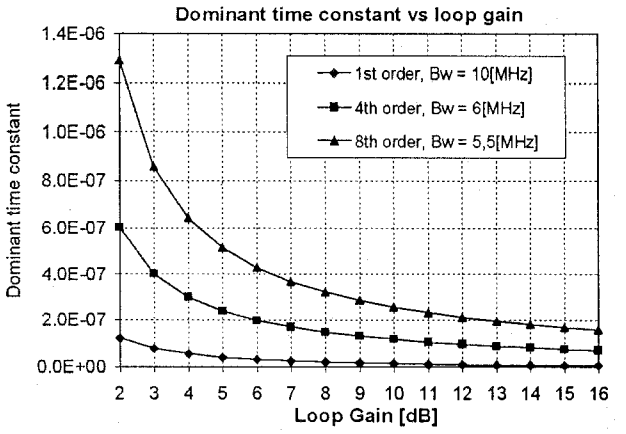

Figure 6: Dominant time constant vs. loop gain

It is instructive to discuss as a reference, the special case of a filter of order one which easily lends itself to an analytical treatment. Figure 7 shows the circuit being considered.

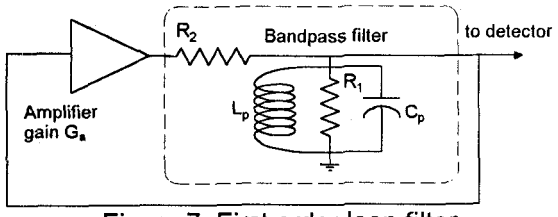

Figure 7: First order loop filter

A very simple analysis yields that the filter bandwidth Bw is

$$Bw = \frac{R_1 + R_2}{(R_1 R_2) \cdot 2\pi C_p} \tag{16}$$

the loop gain G is:

$$G = G_a \frac{R_1}{R_1 + R_2} \tag{17}$$

and the time constant τ is:

$$\tau = \frac{1}{\pi Bw(G-1)} \tag{18}$$

Thus for the first order filter, the time constant depends inversely on the bandwidth, a behavior that as observed in figure 5 holds for higher order Butterworth filters as well. It is interesting to see that increasing the order of the filter has the same effect on the time constant as narrowing the bandwidth of a first order filter. For a first order loop, (18) defines the relation between loop gain, filter bandwidth and the resulting time constant. The order of the filter adds an additional degree of freedom in the design process, allowing a more flexible choice of gain or filter bandwidth for a given value of τ. It can also be seen from figure 6, that whatever the order of the filter, the sensitivity of τ to gain variations is much less significant for high loop gains. Thus in a practical design, which should be as insensitive as possible to component tolerances and thermal variation of parameters, the choice of G will be restricted to values considerably larger than the minimum required for oscillation.

An important consequence of the above results is the fact that the maximum possible quench frequency does not only depend on the filter bandwidth but also on it's order. Thus, for a given bandwidth, the first order loop allows the use of the highest possible quench frequency. In the next section we will show how the presence of delay lines in the loop also influences the choice of the quench frequency.

5. DELAY LINES IN LOOP

A fairly recently discussed [6] variation of the basic design incorporates a SAW narrow band delay line in the loop, which successfully deals with the inherent instabilities of RLC based filters. A very interesting result of this modification which is not discussed in [6], is that it adds a degree of freedom in the design, much as does changing the order of the loop filter. The block diagram in figure 8 is the same as shown in figure 1, the only change being the added delay. The narrowband characteristic of the delay device is represented by the loop filter.

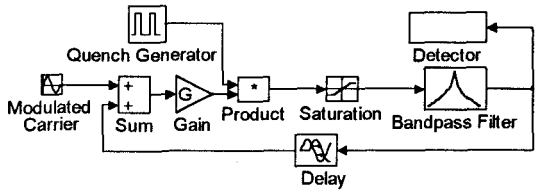

Figure 8: Loop with delay

It is very difficult to determine the behavior of this circuit in general, since it's response cannot be characterized exactly by a rational transfer function, as is possible without the delay. It is of course true in general that the presence of the delay will slow the oscillation buildup in a manner that should be similar to narrowing the bandwidth or increasing the order of the filter. To verify this, small delays were approximated using a 10th order Padé approximation. The value of the dominant time constant was calculated as before for various values of the loop gain, and compared with the corresponding value for a system with no delay. It was found again, that there will normally be a single pair of complex conjugate poles that dominate the response, and thus the growth of the pulses can be very closely approximated by an exponential function. As will be discussed in section 7, simulations of the circuit confirmed that the receiver behavior is equivalent to using a narrower bandpass filter.

A special case can be discussed through an approximate analytical treatment. Let us assume that the (open loop) time constant of the filter is much smaller than the delay. Then, once the feedback loop is closed by the quench signal, the filter output stabilizes at it's steady state step response to the input signal, before the delayed and amplified output is fed back to the input. Once the delayed signal is applied at the input, the cycle repeats, until saturation limits the growth.

Let D be the delay and G the loop gain. Then if the input voltage is V_{in}, D seconds after the loop is closed a voltage GV_{in} will be added to the input which will reach a value $V_{in}(1+G)$. After another D seconds the process repeats and the input signal becomes $V_{in}(1+G+G^2)$. Repeating this argument it is easy to see that the growth curve of an oscillation pulse will be described by :

$$s(nD) = V_{in}\frac{G^{n+1}-1}{G-1} \approx V_{in}\frac{G^{n+1}}{G-1} \quad \text{if } n >> 1 \qquad (19)$$

For t = nD it can be shown that the above equation can be rewritten as:

$$s(t) \approx \frac{V_{in}G}{G-1}e^{\frac{\ln(G)}{D}t} \qquad (20)$$

It follows from (20) that the oscillation pulses will approximately follow an exponential growth curve with a time constant of D/ln(G). Therefore the demodulated output can be calculated approximately by:

$$V \approx f_q E_{max}\frac{D}{\ln(G)}\ln\left(\frac{1+m}{1-m}\right) \qquad (21)$$

Using (13) the bound on the quench frequency now becomes:

$$f_q < \frac{2\ln(G)}{D\ln(\frac{E_{sat}}{E_{min}})} \qquad (22)$$

In the case of a loop with a large delay, the quenching of the oscillations will take a much shorter time than the buildup, as only the latter is affected by the delay. Thus the maximum possible quench frequency can be determined considering (22).

If the filter response is not fast enough to be negligible with regard to the loop delay, then the growth of the pulse waveform will be slower than described by (20) and the quench frequency will have to be reduced with regard to the bound defined by (22).

6. INFLUENCE OF QUENCH WAVESHAPE

It has been shown [3], [4] that modifying the shape of the quench waveform, in the sense of making the transition from the quench to the oscillation condition more gradual, improves the selectivity of the circuit. It has also been claimed [5] that this increases the demodulation gain. A quench waveform chosen for this purpose could be trapezoidal, with long enough periods of constant high gain and zero gain, to allow for full oscillation buildup and full quench. A typical situation is illustrated in figure 9. We will show that in fact, over a wide range of conditions the demodulated voltage is practically independent of the quench waveform.

Let q(t) be the quench waveform, and let T be it's period. We shall assume that q(t) can be described as:

$$q(t) = \begin{cases} f_1(t) & \text{for } 0 < t \le t_1 \\ 1 & \text{for } t_1 < t \le t_2 \\ f_2(t) & \text{for } t_2 < t \le t_3 \\ 0 & \text{for } t_3 < t \le T \end{cases}$$

where $0 < t_1 < t_2 < t_3 < T$ and $f_1(t) \le 1$, $f_2(t) \le 1$

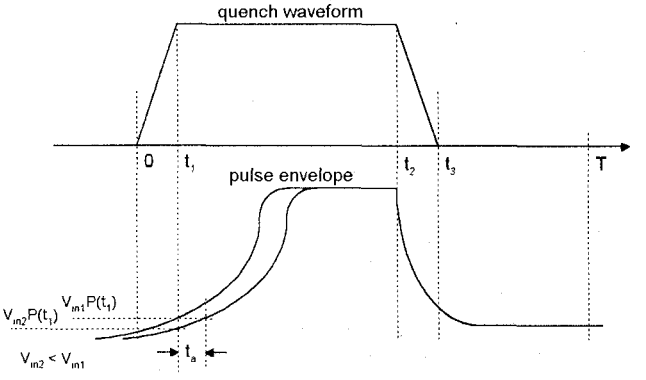

Figure 9: quench and pulse envelope waveforms

We will assume that the quench phase, which starts at t_2 with the decay of q(t), is such that at time T the oscillation has dropped to levels that are much less than the input voltage. Let V_{in} be the amplitude of the sinusoidal input signal at time t = 0. Then assuming that saturation does not occur before t_1, from t = 0 to t = t_1 the circuit behaves as a linear, time varying system. In contrast, from t = t_1 until saturation sets in, the circuit behaves as a linear, time invariant system. Thus at time t_1 the amplitude of the response to V_{in} can be written as $V_{in}P(t_1)$, where the function P(t) depends on the shape of $f_1(t)$. For any reasonable quench waveform $P(t_1)$ will be greater than one. We will assume however that $V_{in}P(t_1)$ is much smaller than the pulse saturation voltage. From time t_1 on, the amplitude of the oscillation will grow exponentially until saturation sets in, exactly as happens with rectangular quench. Under the above conditions it will be true that the area under the pulse envelope will practically only depend on the behavior of the exponential growth phase, and thus on it's initial condition $V_{in}P(t_1)$, and

not on the behavior before t_1. In terms of the analysis presented in [5] this means that the time of advance t_a used for the calculation of the change in area under the pulses depends on the behavior of the oscillation after t_1, and not before this time as indicated in [5]. This reduces the problem to the one solved for rectangular quench, with input amplitudes given by $V_{in}P(t_1)$ instead of V_{in}. But for rectangular quench the demodulated output is independent of the input voltage as long as saturation occurs. It is then clear that under the stated conditions the quench waveshape does not affect the demodulated output voltage.

It is obviously possible to find special conditions under which the above will not hold. For a given q(t) this will happen if the oscillation pulses approach saturation levels before t_1 (very strong input signals) or if the pulses do not reach saturation at all (very weak input signals). In the first case, the area under the pulse envelope becomes dependent on its behavior before t_1. As during this interval the rate of growth is smaller than during the constant gain phase, an increase of the time of advance, and consequently of the demodulated voltage is to be expected.

A different situation arises for weak input signals, such that pulses do not reach saturation. As in the rectangular quench case, amplitude modulation of the pulses sets in as the signal input level weakens. For input levels such that the pulse amplitude still comes close to saturation, the result is a rise in demodulated output, due to the combination of pulse amplitude and width modulation. Further decreases in input signal level reduce the amplitude of the oscillation pulses, and as a result the demodulated output drops. While this behavior is common to any quench waveform, under rectangular quench conditions it occurs when the oscillation pulses are very narrow, and thus the effect of the amplitude modulation is not significant. For a more gradual transition from oscillation to quench, the growth and decay rate of the pulses is reduced. This implies that as the input level decreases, the point where amplitude modulation sets in is reached earlier. (i.e. at stronger signal levels). Also the decrease in pulse growth and decay rate implies an increase in the pulse area and thus in a stronger effect of the amplitude modulation. Thus a larger increase in demodulated voltage, at a higher input level is to be expected for a quench waveform that departs from the rectangular shape.

Another aspect that must be taken into account is that the slower growth and decay of the oscillation pulses for non-rectangular quench will result in the need for a lowering of the quench frequency, or in an increase of the minimum input signal level that assures saturation.

As will be seen in the next section this behavior has been confirmed by the results of simulation.

7. SIMULATION RESULTS

The results of the analysis presented above have been compared with those of extensive computer simulations of the superregenerative receiver. Most simulations were performed on TESOFT'S TESLA simulator for PC type computers. As is usually necessary for modulated carrier systems the carrier frequency was scaled down to much lower values than would be used in practice, to avoid the need for an excessive number of simulation points. A very large number of different situations were simulated, among which we only include those that are the most relevant.

The basic configuration considered corresponds to the model of figure 1, having the following parameters:

Loop Gain: variable between 2.2[dB] and 16[dB]
Quench frequency: variable between 1[kHz] and 5[kHz].
Amplifier: 1[dB] compression point: 10[dBm] *Loop filter*: Butterworth and Chebycheff filters of various orders; center frequency 1[MHz], bandwidth variable between 40[kHz] and 120[kHz].
Detector: Envelope detector followed by fourth order Butterworth low pass filter.
Input signal level: variable from less than 1[nV] to 10[mV]
Amplitude modulation index: 0.5
Modulating signal: sinusoid of frequency less than 1/20 of quench frequency.

In all cases simulated, the parameters were chosen in such a way that saturation of the pulses occurred, and during the quench phase the pulse level dropped below the input signal voltage.

7.1 Constant demodulated output

The property of constant demodulated output of the receiver was tested for a large variety of conditions, including Butterworth and Chebycheff filters of orders up to eight, and loops with or without delays. In all cases the simulated receiver exhibited a constant output as long as the quench frequency was chosen

such as to assure complete saturation and quenching.

7.2 Influence of loop gain

The effect of the loop gain on the demodulated output was determined for a first order loop with a bandwidth of 100[kHz], a quench frequency of 5[kHz], average input signal 1[μV], the remaining parameters being chosen as defined above. The theoretical curve was obtained using (2), (14) and (18). Figure 10 shows the results obtained.

As can be seen there is a very good match between the simulation results for the receiver and the theoretical expression. The difference at low gains is due to the fact that the validity of (14) requires high loop gains. If the real values of E_{max}, obtained from the simulation, are used instead of the estimate based on (14), the error becomes negligible. Simulations for a wide range of input signal levels yield, as expected, exactly the same results. It was also confirmed, that as discussed in section 4, with an appropriate scale factor, the behavior of loops with higher order filters is quite close to the curve in figure 10. The scale factor corresponds to the reduction in quench frequency necessary to compensate for the longer time constant associated with the higher order filter. It is also worth mentioning that simulations with other types of filters, such as Chebycheff filters of various orders, yield the same type of behavior.

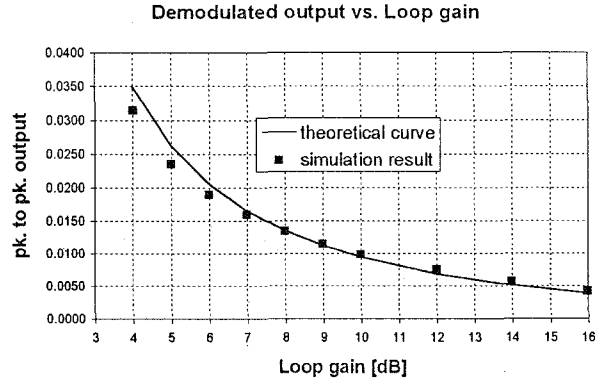

Figure 10: Demodulated voltage vs. loop gain

7.3 Effect of filter order and bandwidth

The analysis presented in section 4 indicates that an increase in the order of the filter results in an increase of the time constant τ (and thus of the demodulated voltage), the same effect being possible through a loop gain reduction for the first order loop. The discussion of the behavior of the closed loop also indicates, that the dependency of τ on the inverse of the bandwidth, obtained analytically for first order filters, holds for higher order filters as well.

The results of extensive simulations have confirmed this analysis. The following figures show the behavior of two receivers: one uses a first order filter with a loop gain of 2.2[dB] while the other includes a fourth order filter and a loop gain of 6[dB].

As can be seen, both exhibit practically identical behaviors as well as an excellent match to the theoretical curve for a first order loop defined by (2), (14) and (18). In addition, simulations of receivers that include a Chebycheff filter instead of a Butterworth filter were performed. Again the same results were obtained. For example a receiver with a Chebycheff filter of order 2, a ripple of 2[dB] and a loop gain of 4.2[dB] was found to have exactly the same output vs. bandwidth curve of the first order loop with gain 2.2[dB]

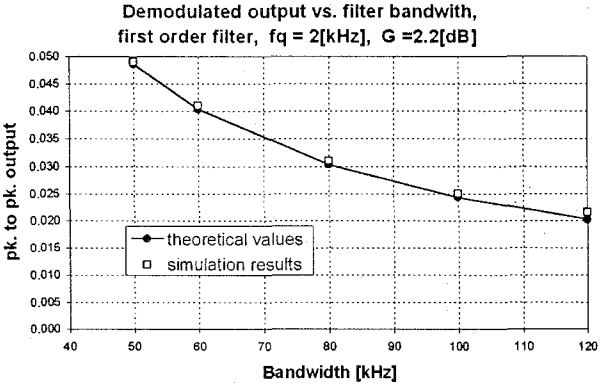

Figure 11: Influence of loop bandwidth, first order filter

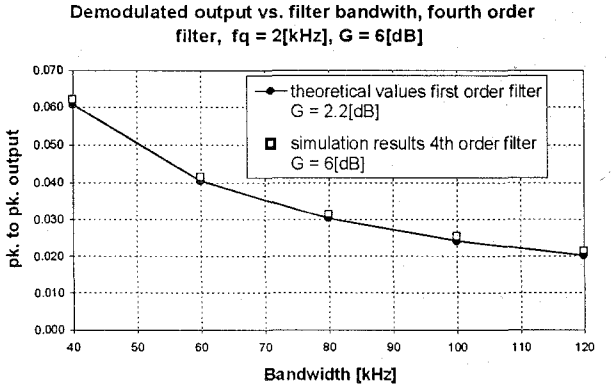

Figure 12 : Influence of loop bandwidth, fourth order Butterworth filter

7.4 Influence of delays in the loop

Two types of situations were considered. First the receiver was simulated considering delays comparable to a carrier period, as would for example be necessary in practice, to compensate for a phase shift of the amplifier. As predicted by the analysis, the result was a longer time constant and exponential growth of the oscillation pulses, resulting in constant demodulated output over a wide range of input signal levels. The behavior of the receiver is essentially equivalent to that obtained through use of a higher order filter.

For the case of loops that include a long time delay compared to the filter time constant, an approximate treatment was presented in section 5. Simulations of this situation indicate that the approximate model, characterized by (14) and (21) permits a quite accurate prediction of the receiver's behavior. The following figures illustrate some typical results.

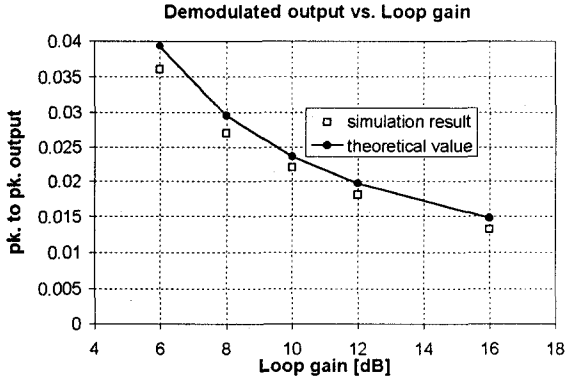

Figure 13: Demodulated output vs. loop gain for bandwidth = 200[kHz], delay = 21[μsec]

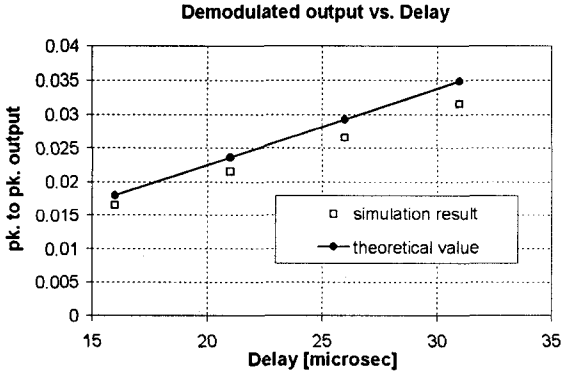

Figure 14: Demodulated output vs. delay for loop gain = 10[dB], bandwidth = 200[kHz],

In both cases the difference between the simulated results and the theoretical values are due basically to the inaccuracy incurred in estimating E_{max} by use of (14). If the actual value of E_{max} observed in the simulation is used, the error becomes negligible.

7.5 Influence of quench waveform

The treatment presented in section 6 indicates that the increase in demodulated output due to a trapezoidal quench waveform, mentioned in the literature [5], will only happen for a limited range of input signal levels. This behavior was confirmed through extensive simulations. Figure 15 illustrates the behavior of a receiver with a first order filter, under two quench conditions, rectangular and trapezoidal.

The trapezoidal quench condition has been chosen as a rather extreme case, to emphasize the behavior: A triangular waveform with an average value of 0.5 and a peak to peak value of 1.4 was clipped at the levels 1 and 0. It is clearly seen that as expected, the trapezoidal quench significantly reduces the input level range that results in a constant demodulated output. In any practical application, the extremely low input levels simulated for rectangular quench, would certainly be useless, due to the presence of circuit noise and interference. The purpose of this analysis is however to show that a trapezoidal quench does not improve demodulated output, except in a particular input level range, and that it has the disadvantage of narrowing the region where a constant output level can be expected.

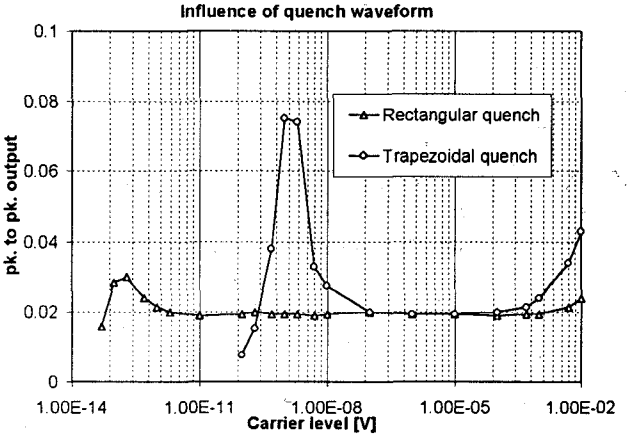

Figure 15: Demodulated peak to peak output voltage for rectangular and trapezoidal quench conditions.

8. CONCLUSIONS

A model for the superregenerative receiver, based on a block diagram approach has been obtained and validated through extensive simulation. The model clarifies the complex interrelation between the various design parameters, and takes much of the guesswork out of the design procedure. While only certain configurations were discussed, the analysis and simulation tools used are general and can be applied to a wide range of cases.

With regard to specific results, it was shown that the constant demodulated output property of the receiver will hold for virtually any configuration. The relationship between demodulated output, loop gain and filter parameters was obtained for the simple first order case, and generalized to more complex situations, using computer based tools to determine the behavior of the closed loop poles. The effect of the quench waveshape was discussed, and it was shown that as long as saturation occurs it has little influence on the demodulated output. Many other points relating to the design of the superregenerative receiver, such as the very important aspect of selectivity, can be addressed with the aid of the computer based tools that were used in this work.

BIBLIOGRAPHY

[1] Edwin H. Armstrong, "Some Recent Developments on Regenerative Circuits"; *Proceedings of the IRE*, 10, August 1922.

[2] Frink, Frederick W. "The Basic Principles of Superregenerative Reception" *Proc. of the IRE.*, Vol. 26 No. 1 October 1944, pp. 76-106

[3] Bradley, William E. "Superregenerative Detection Theory", *Electronics*, Sept. 1948, pp. 96-98.

[4] Hazeltine, Alan Richman, D. & Loughlin, B.D. "Superregenerator Design", *Electronics*, Sept. 1948, pp. 99-102.

[5] "Microwave Receivers", Edited by S.N. Van Voorhis, Dover Publications, New York, 1966. Ch. 20 "Superregenerative Receivers".

[6] Ash, Darrell L.. "A Low Cost Superregenerative SAW Stabilized Receiver" IEEE Transactions on Consumer Electronics, Vol CE-33, No. 3, August 1987 pp. 395-403

[7] Mc Coy, William G. "Design of a Superregenerative Receiver for Solar Powered Applications" IEEE Transactions on Consumer Electronics, Vol CE-38, No. 4, November 1992 pp. 869-873.

[8] Darrell Ash and Lon Cecil, RF Monolitics Inc. Personal communication, November 1995.

Acknowledgments

This work was supported by Research Grant No. 1950943 from the Fondo Nacional de Investigación Científica y Tecnológica (FONDECYT)

Rodolfo Feick received the degree of Ingeniero Civil Electrónico from Universidad Técnica Federico Santa María in 1970; the M. Sc. in Electrical Engineering from the University of Pittsburgh in 1972 and the Ph. D. in Electrical from the University of Pittsburgh in 1975. He is a Professor for Electronics Engineering at Universidad Técnica Federico Santa María, head of the Telecommunications Group, and a Senior Member of the IEEE.

Osvaldo Rojas received the degree of Licenciado en Ciencias de la Ingeniería from Universidad Técnica Federico Santa María in 1995. He is currently completing the requirements for the M. Sc. degree and the Ingeniero Civil Electrónico degree, at the Department of Electronics Engineering of Universidad Técnica Federico Santa María.

Alejandro Mackay received the degree of Ingeniero Civil de Industrias from the Pontificia Universidad Católica de Chile in 1972 and the Ph. D. in Electrical from the University of Alberta in 1977. He is a Professor for Electronics Engineering at the Pontificia Universidad Católica de Chile